

## การประเมินป่าในเมืองด้วยการรับรู้ระยะไกล ผ่านเทคโนโลยีอวกาศ: มวลชีวภาพและการกักเก็บคาร์บอน

ชนกฤต พิบบขุนทด<sup>1</sup> อีรวงศ์ เหล่าสุวรรณ<sup>2,3\*</sup> ญาณวุฒิ อุทร์ักษ์<sup>3,4\*</sup>  
สาธิต แสงประดิษฐ์<sup>3,5</sup> ธนัทเดช โรจนกุล<sup>2,3</sup> วุฒิศักดิ์ บุญแน่น<sup>1</sup> และองอาจ ญาตินิยม<sup>1</sup>

วันที่รับ 13 สิงหาคม 2568 วันที่แก้ไข 27 สิงหาคม 2568 วันที่ออกรับ 28 สิงหาคม 2568

### บทคัดย่อ

การเปลี่ยนแปลงสภาพภูมิอากาศซึ่งซับซ้อนขึ้นโดยการเพิ่มขึ้นของก๊าซคาร์บอนไดออกไซด์ในบรรยากาศ ได้กลายเป็นความท้าทายระดับโลก งานวิจัยนี้มีวัตถุประสงค์เพื่อประมาณการมวลชีวภาพเหนือพื้นดิน และปริมาณคาร์บอนสะสมของต้นไม้ในเขตเมือง โดยใช้ข้อมูลภาพถ่ายดาวเทียม Sentinel-2 ซึ่งเป็นเทคโนโลยีอวกาศร่วมกับการสำรวจภาคสนาม มีการจัดตั้งแปลงตัวอย่าง 30 แปลง ขนาด 20 x 20 เมตร เพื่อเก็บข้อมูล และคำนวณดัชนีพืชพรรณพร้อมสัดส่วนพื้นที่ปกคลุมจากข้อมูลดาวเทียม จากนั้นใช้สมการอัลโลเมตริกในการประเมินมวลชีวภาพเหนือพื้นดินและการกักเก็บคาร์บอน พร้อมวิเคราะห์ความสัมพันธ์ระหว่างมวลชีวภาพเหนือพื้นดินและค่าดัชนีพืชด้วยสมการถดถอย เอกซ์โพเนนเชียล ผลการวิเคราะห์พบว่า GNDVI เป็นดัชนีที่มีประสิทธิภาพสูงสุด การสำรวจภาคสนามระบุมวลชีวภาพเหนือพื้นดินรวม 4,650.75 ตัน และคาร์บอน 2,185.85 ตัน ขณะที่การประเมินด้วยดาวเทียมให้ค่า 2,798.23 ตัน และคาร์บอน 1,315.17 ตัน ตามลำดับ ผลลัพธ์ยืนยันถึงประโยชน์ของการบูรณาการเทคโนโลยีอวกาศร่วมกับข้อมูลภาคสนาม เพื่อการประเมินมวลชีวภาพและคาร์บอนในเขตเมืองอย่างแม่นยำ เป็นการสนับสนุนการวางแผนพื้นที่สีเขียว การจัดการทรัพยากรธรรมชาติ และการบรรเทาผลกระทบจากการเปลี่ยนแปลงสภาพภูมิอากาศ

**คำสำคัญ :** เทคโนโลยีอวกาศ, บริการระบบนิเวศ, ป่าในเขตเมือง, มวลชีวภาพเหนือพื้นดิน, ปริมาณคาร์บอนสะสม, สมการอัลโลเมตริก

<sup>1</sup> โรงเรียนสาธิตมหาวิทยาลัยมหาสารคาม (ฝ่ายมัธยม) มหาวิทยาลัยมหาสารคาม จังหวัดมหาสารคาม 44150

<sup>2</sup> ภาควิชาฟิสิกส์ คณะวิทยาศาสตร์ มหาวิทยาลัยมหาสารคาม จังหวัดมหาสารคาม 44150

<sup>3</sup> ศูนย์วิจัยและปฏิบัติการก๊าซเรือนกระจก คณะวิทยาศาสตร์ มหาวิทยาลัยมหาสารคาม จังหวัดมหาสารคาม 44150

<sup>4</sup> ภาควิชาชีววิทยา คณะวิทยาศาสตร์ มหาวิทยาลัยมหาสารคาม จังหวัดมหาสารคาม 44150

<sup>5</sup> ภาควิชาภูมิสารสนเทศ คณะวิทยาการสารสนเทศ มหาวิทยาลัยมหาสารคาม จังหวัดมหาสารคาม 44150

\* ผู้ประพันธ์บรรณกิจ, อีเมล: teerawong@msu.ac.th, yannawut.u@msu.ac.th

# Remote Sensing of Urban Forest Estimation via Space Technology: Biomass and Carbon Storage

Thanakrizt Peebkhunthod<sup>1</sup> Teerawong Laosuwan<sup>2,3\*</sup> Yannawut Uttaruk<sup>3,4\*</sup>  
Satith Sangpradid<sup>3,5</sup> Tanutdech Rotjanakusol<sup>2,3</sup> Wutthisak Bunnaen<sup>1</sup> and Ongart Yatniyom<sup>1</sup>

Received 13 August 2025 Revised 27 August 2025 Accepted 28 August 2025

## Abstract

Climate change, largely driven by rising atmospheric carbon dioxide, presents urgent global challenges. This study estimated aboveground biomass (AGB) and carbon stock of urban trees using space technology Sentinel-2 satellite imagery from combined with field surveys. Thirty 20 × 20 m plots were established for data collection, and vegetation indices with fractional cover were derived from satellite data. Allometric equations were applied to estimate AGB and carbon stock, while exponential regression examined the relationship between biomass and vegetation indices. Results showed GNDVI as the most effective index. Field surveys indicated 4,650.75 tons of AGB and 2,185.85 tons of carbon, whereas satellite-based estimates yielded 2,798.23 tons and 1,315.17 tons, respectively. These findings demonstrate the benefits of integrating space technology with field measurements for reliable assessment of urban biomass and carbon storage. The approach provides useful insights for urban green space planning, natural resource management, and strategies to mitigate climate change.

**Keywords:** space technology, ecosystem services, urban forest, aboveground biomass, carbon stock

---

<sup>1</sup> Maharakham University Demonstration School, Maharakham University, Maha Sarakham, 44150, Thailand.

<sup>2</sup> Department of Physics, Faculty of Science, Maharakham University, Maha Sarakham, Thailand.

<sup>3</sup> Greenhouse Gas Research Center and Operations, Maharakham University, Maha Sarakham 44150, Thailand.

<sup>4</sup> Department of Biology, Faculty of Science, Maharakham University, Maha Sarakham, Thailand.

<sup>5</sup> Department of Geoinformatics, Faculty of Informatics, Maharakham University, Maharakham 44150, Thailand.

\* Corresponding author: teerawong@msu.ac.th, yannawut.u@msu.ac.th

## 1. Introduction

At present, climate change and the increase in greenhouse gases have become major global issues, receiving significant attention worldwide [1]. One of the primary factors contributing to global warming is the emission of carbon dioxide (CO<sub>2</sub>) into the atmosphere [2]. These emissions originate from various sources, including the combustion of fossil fuels in industry, transportation, and everyday energy consumption [3,4]. The rise in global temperatures has caused drastic climate changes, severely affecting biodiversity [5]. Many animal and plant species are facing habitat alterations, with some potentially becoming extinct due to their inability to adapt to rapid changes [6]. Moreover, climate change has degraded ecosystems, disrupting the natural balance essential for the survival of all living organisms [7]. In addition, rising temperatures and unpredictable weather patterns negatively affect agriculture. Previously productive cultivation may suffer from unseasonal rainfall or droughts, forcing farmers to adapt and seek new, climate-resilient crops [8]. Furthermore, global warming adversely impacts human health, increasing the incidence of heat-related illnesses and air pollution-related diseases [9].

Utilizing ecosystem services, such as urban tree planting, offers an effective means of climate change adaptation. Trees not only sequester carbon but also mitigate urban heat, enhance biodiversity, and improve air and water quality [10]. Moreover, urban trees contribute to creating a more livable

environment, reducing stress, and promoting mental well-being among city residents [11]. Promoting urban tree planting is one potential solution to climate change, and requires systematic planning and management of green spaces to maximize ecosystem service benefits provided by trees [12]. Aboveground biomass (AGB) is considered one of the most effective carbon sinks, as plants absorb atmospheric carbon dioxide and convert it into organic carbon stored within their tissues [13]. Assessing AGB and carbon sequestration in various areas enhances our understanding of the carbon storage potential of vegetation and supports the planning of sustainable natural resource management [14]. Increasing AGB also plays a role in reducing urban temperatures and creating livable environments for communities [15]. Generally, the amount of carbon stored in trees correlates directly with biomass, which represents the total mass of all tree components, including stem, branches, leaves, and roots [16]. Therefore, anatomical characteristics of trees—such as height, trunk diameter, and canopy width—can be used to estimate stored carbon using allometric equations, which establish relationships between biomass and tree structure [17].

Remote sensing powered by space technology provides an efficient method that reduces both labor and time needed for field surveys. [18,19]. This technology can be applied to assess biomass and carbon sequestration [20]. It utilizes satellite imagery and aerial photographs to analyze large areas with precision and speed,

enhancing the efficiency and cost-effectiveness of surveys [21]. Furthermore, remote sensing technology can monitor long - term biomass changes and allow accurate and timely evaluation of resource management impacts and related policies. Therefore, the study of biomass and carbon sequestration is not only academically important but also practically significant. This study aims to estimate the aboveground biomass and carbon stock of urban forests using Sentinel-2 imagery integrated with field measurements. The study provides new insights into the role of vegetation indices in urban biomass modeling and offers policy-relevant implications for green space planning and carbon credit assessment.

## 2. Materials and Methods

### 2.1 Study Area

The study area for this research on urban tree carbon stock was selected to be Mahasarakham University (Figure. 1).

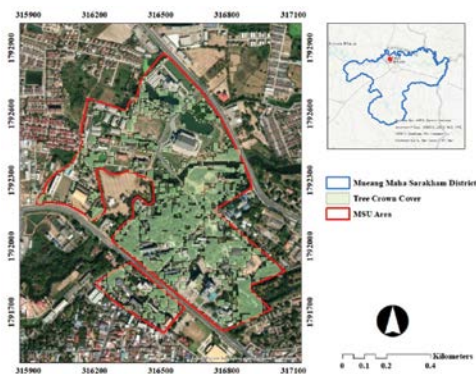


**Figure 1** Study area

Mahasarakham University located in Talat Sub-district, Mueang Mahasarakham District, Mahasarakham Province, at the coordinates 3164.71.52 E and 1791741.78 N. Mahasarakham Province is characterized by generally flat to gently undulating terrain, with elevations ranging between 130 - 230 meters above sea level. The climate is classified as Tropical Monsoon Climate. During the summer monsoon season, the province receives southwesterly monsoon winds from the Indian Ocean. The climate exhibits alternating wet and dry periods. The annual average temperature is 27.4°C, with an average minimum of 22.4°C and an average maximum of 33.7°C. April is typically the hottest and most humid month of the year.

### 2.2 Field data collection

Field data collection involved identifying tree species and measuring the dimensions of all trees with a diameter at breast height (DBH), measured at 1.30 meters above the ground, greater than 4.5 centimeters. Data were collected from 30 sample plots, each measuring 20 × 20 meters. DBH was measured using a diameter tape, and tree height (H) was measured using a laser rangefinder. Tree growth analysis focused on two primary parameters: DBH and height (H), which provide essential insights into various aspects of tree development. Upon obtaining growth data, aboveground biomass (AGB) was calculated using allometric equations (Equation 1) [22], which convert growth metrics into biomass

estimates. Following this, AGB values were utilized to calculate carbon stock through Equation 2. To assess carbon stock, we transformed the AGB into carbon stock by applying the IPCC's suggested default wood carbon factor of 0.47, which signifies that 47% of the dry mass of all above-ground tree parts is composed of [23]. The application of allometric equations and carbon estimation is a critical process for understanding the environmental contribution of urban trees.

$$\begin{aligned} W_S &= 0.0396(D^2 H)^{0.933} \\ W_B &= 0.00349(D^2 H)^{1.030} \\ W_L &= \left( \frac{28}{W_S + W_B} + 0.025 \right)^{-1} \\ W_T &= W_S + W_B + W_L \end{aligned} \quad (1)$$

$D$  denotes the diameter at breast height (cm),  $H$  the tree height (m),  $W_S$  the stem biomass (t/ha),  $W_B$  the branch biomass (t/ha), and  $W_L$  the leaf biomass (t/ha)

$$C_j = W_{tc} \times FC \quad (2)$$

$C_j$  denotes the carbon storage potential of a tree (kg),  $W_{tc}$  represents the aboveground biomass (kg), and  $FC$  is the carbon fraction of biomass, fixed at 0.47.

### 2.3 Satellite Data Analysis

Sentinel-2 imagery obtained on October 4, 2024, was employed in this study to compute vegetation indices, namely the Normalized Difference Vegetation Index (NDVI) [24] and the Green Normalized Difference Vegetation

Index (GNDVI) [25], using the formulas in Equations 3 and 4. These indices were then used to derive the Fractional Green Vegetation Cover (FC) as defined in Equation 5 [26]. The use of vegetation indices is particularly valuable in assessing vegetation status, including tree density and overall health of vegetated areas.

$$NDVI = \frac{NIR - RED}{NIR + RED} \quad (3)$$

The widely recognized NDVI is a straightforward yet powerful index for measuring green vegetation. It compares the scattering of green leaves in the Near Infrared spectrum with the absorption of chlorophyll in the red spectrum. The NDVI values range from -1 to 1. Negative NDVI values (approaching -1) are indicative of water bodies. Values near zero (-0.1 to 0.1) typically represent barren landscapes such as rock, sand, or snow. Low positive values suggest the presence of shrub and grassland (approximately 0.2 to 0.4), while high values signify temperate and tropical rainforests (values nearing 1).

$$GNDVI = \frac{NIR - GREEN}{NIR + GREEN} \quad (4)$$

The Green Normalized Difference Vegetation Index (GNDVI) measures the greenness and photosynthetic activity of plants. It is a commonly utilized vegetation index for assessing water and nitrogen absorption within the crop canopy. The index values

range from -1 to 1, where values between -1 and 0 indicate the presence of water or bare soil. This index is primarily applied during the intermediate and final stages of the crop growth cycle.

$$FC = \frac{NDVI - NDVI_{soil}}{NDVI_{veg} + NDVI_{soil}} \quad (5)$$

Fractional Green Vegetation Cover (FC) serves as a crucial parameter in climate modeling. Remote sensing technology has emerged as one of the most efficient methods for obtaining information on vegetation dynamics. The model presumes that a given pixel is composed of green vegetation and bare soil, leading to the conclusion that the NDVI value is a linear combination of NDVI<sub>veg</sub> and NDVI<sub>soil</sub>. Typically, NDVI<sub>veg</sub> is identified as the highest NDVI [27], while NDVI<sub>soil</sub> is derived from the lowest NDVI observed in the scene (Yang et al., 2006). Numerous studies reference commonly accepted NDVI<sub>soil</sub> values of 0.05 or lower [28]. Nevertheless, images are often affected by noise, which means that the maximum and minimum NDVI values in an image may not accurately represent NDVI<sub>veg</sub> and NDVI<sub>soil</sub>.

## 2.4 Correlation Analysis

The relationship between Fractional Green Vegetation Cover (FC) and AGB density was examined through an exponential regression model, which proves to be efficient in estimating biomass using Sentinel-2 satellite data. The standard equation format is presented in Equations 6.

$$AGB = a \times b^{e \times FC} \quad (6)$$

The constants a and b are established based on field data and vegetation indices. The analysis indicated that biomass generally increases exponentially as vegetation cover rises.

## 2.5 Statistical Validation Using Root Mean Square Error (RMSE)

In order to present a succinct overview of this study, the methodology is outlined in a series of sequential steps as detailed below. This research centers on the examination of the Normalized Difference Vegetation Index (NDVI) through the utilization of monthly data obtained from Terra/MODIS satellite imagery. The first step entails the computation of the raw NDVI values as defined by Equation 1, followed by multiplying the results by 0.0001 to obtain more accurate values. After calculating the NDVI values, the coordinates are transformed to the WGS 1984 UTM Zone 47N system to ensure precision in map location. Subsequently, the study employs conditional sampling to select the largest cultivated areas of four types of economic crops: rice fields, fruit trees, perennial trees, and field crops.

This sampling approach prioritizes large areas to facilitate data analysis and efficiently monitor changes in cultivated areas. The sampling process is conducted for each district in Nong Bua Lam Phu Province, ultimately leading to the creation of graphs

that display the NDVI values derived from this analysis. The accuracy of the biomass estimation model was evaluated using Root Mean Square Error (RMSE) (Equation 7), which quantifies the deviation between predicted and observed values. RMSE is calculated by taking the square root of the mean of the squared differences between the model's predicted values and actual field measurements. A lower RMSE indicates higher model accuracy and lower prediction error. In this case study, where AGB was estimated using satellite-derived vegetation indices, RMSE serves as an important metric to assess model reliability and improve its accuracy based on the available data. Therefore, RMSE plays a vital role in validating the model's predictive performance.

$$RMSE = \sqrt{\frac{1}{n} \sum_{i=1}^n (AGB_{pred} - AGB_{obs})^2} \quad (7)$$

*AGB<sub>pred</sub>* represents the estimated biomass value derived from the vegetation index, while refers to the biomass value obtained from field data, with n indicating the number of samples.

### 3. Results and Discussions

#### 3.1 Analysis of Tree Physical Characteristics

Field surveys were conducted from October 4 to 5, 2024, during the late rainy season, which provided optimal conditions for efficient field data collection. Key measurements recorded included diameter at breast height (DBH) and tree height (H), along with the use

of Global Positioning System (GPS) to record the location of each sample plot. The AGB was calculated using allometric equations, and the results are presented in Table 1. This variation emphasizes the key role of large trees in overall biomass accumulation and highlights the structural diversity that must be considered in urban forest assessments. Such heterogeneity provides essential context for accurate biomass estimation and carbon stock evaluation. In particular, differences in canopy structure and species composition can significantly influence biomass distribution across plots. These factors reinforce the need for site-specific approaches when applying remote sensing or modeling techniques to urban forest ecosystems.

The variation in the AGB among plots reflects differences in tree size and structure. Plot 19 and Plot 21 recorded unusually high biomass values, mainly due to the presence of large-diameter and tall trees, which strongly influence the allometric equations applied for estimation. Since DBH and height act as exponential factors in biomass models, a few large individuals can significantly raise the total biomass within a plot. This relationship confirms that tree size remains a reliable predictor of AGB and validates the accuracy of the chosen equations.

These findings emphasize the role of plot-level heterogeneity in shaping carbon storage potential. Mature trees not only increase biomass but also provide valuable ecosystem services such as shading, tem-

**Table 1** Aboveground biomass

Plot	Mean DBH	Mean H	Sum of Aboveground biomass in branch part (kg)	Sum of Aboveground biomass in stem part (kg)	Sum of Aboveground biomass in leaf part (kg)	Sum of Aboveground biomass (kg)	Sum of all above ground biomass (ton/400 m <sup>2</sup> )	Sum of all above ground biomass (ton/ha)
01	21.23	7.23	235.08	1,156.81	49.72	1,441.61	1.44	36.04
02	21.69	5.43	1,079.90	3,949.66	179.64	5,209.20	5.21	130.23
03	22.36	8.23	271.52	1,338.01	57.49	1,667.02	1.67	41.68
04	19.78	7.94	310.43	1,501.53	64.73	1,876.69	1.88	46.92
05	38.48	12.00	1,439.85	5,754.56	256.95	7,451.36	7.45	186.28
06	35.65	10.67	476.37	2,043.86	90.01	2,610.25	2.61	65.26
07	37.40	14.13	1,104.23	4,421.06	197.34	5,722.63	5.72	143.07
08	28.46	10.60	489.38	2,206.36	96.29	2,792.02	2.79	69.80
09	67.48	21.75	2,032.66	7,474.00	339.53	9,846.19	9.85	246.15
10	65.49	17.50	2,023.25	7,208.00	329.69	9,560.95	9.56	239.02
11	58.09	19.50	2,958.65	11,109.71	502.45	14,570.81	14.57	364.27
12	31.19	10.14	600.32	2,424.50	108.04	3,132.86	3.13	78.32
13	7.79	5.74	48.15	271.45	11.43	331.03	0.33	8.28
14	22.18	8.89	456.61	1,939.73	85.59	2,481.94	2.48	62.05
15	35.57	10.25	870.19	3,120.51	142.53	4,133.22	4.13	103.33
16	30.74	13.00	1,181.44	5,036.95	222.10	6,440.48	6.44	161.01
17	14.26	7.21	291.33	1,356.14	58.86	1,706.33	1.71	42.66
18	29.33	10.43	1,116.56	4,031.71	183.87	5,332.14	5.33	133.30
19	27.25	12.13	2,817.58	9,878.23	453.44	13,149.25	13.15	328.73
20	28.03	10.50	905.27	3,824.41	168.93	4,898.61	4.90	122.47
21	87.54	21.00	1,842.89	6,350.37	292.62	8,485.88	8.49	212.15
22	17.54	6.91	113.09	595.72	25.32	734.13	0.73	18.35
23	16.64	7.00	104.51	554.43	23.54	682.49	0.68	17.06
24	54.37	13.20	1,442.02	5,300.96	240.83	6,983.80	6.98	174.60
25	32.20	11.50	700.38	2,761.89	123.66	3,585.93	3.59	89.65
26	43.99	9.80	587.15	2,422.83	107.50	3,117.48	3.12	77.94
27	127.32	15.00	1,231.16	4,195.18	193.80	5,620.14	5.62	140.50
28	25.46	9.77	876.49	3,972.19	173.19	5,021.87	5.02	125.55
29	32.07	8.13	359.79	1,643.35	71.55	2,074.69	2.07	51.87
30	20.51	7.29	213.80	1,085.46	46.41	1,345.68	1.35	33.64
Mean	-	-	-	-	-	-	-	118.34
SD	-	-	-	-	-	-	-	90.14
Variance	-	-	-	-	-	-	-	8125.77

perature regulation, and long-term carbon sequestration. In contrast, plots with lower biomass may represent younger stands requiring targeted management.

### 3.2 Satellite Data Analysis

The results of satellite data analysis using Sentinel-2 were based on three main types of vegetation indices: NDVI, and GNDVI, as illustrated in Figure 2–3 and summarized in Table 2. The analysis revealed clear variations in index values across plots, reflecting differences in canopy density and vegetation vigor. These variations provided the basis for establishing regression relationships with AGB and carbon stock.

The details can be described as follows: Figure 2 (a) presents NDVI values, with a minimum of -0.0339215 and a maximum of 0.678909, while Figure 2 (b) shows the NDVI-derived Fractional Cover, representing the proportion of green vegetation cover, with values ranging from 0.0000 to 99.9999. Figure 3 (a) displays GNDVI values ranging from -0.0339215 to 0.678909 within the Mahasarakham University (MSU) area, which is outlined in red. Figure 3 (b) illustrates the GNDVI-derived Fractional Cover, also ranging from 0.0000 to 99.9999 within the same area.

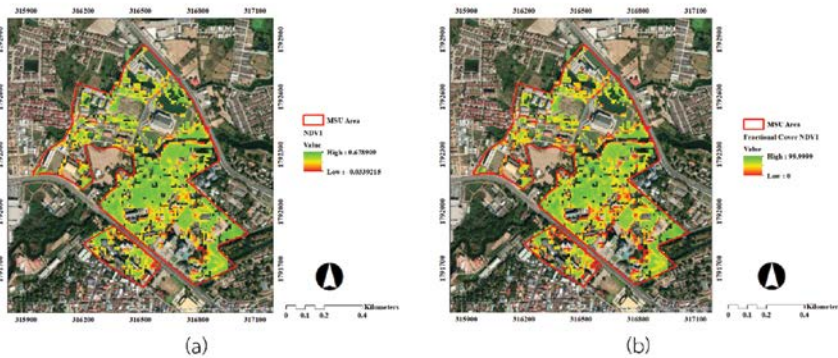


Figure 2 Satellite data analysis (a) NDVI and (b) NDVI-derived Fractional Cover

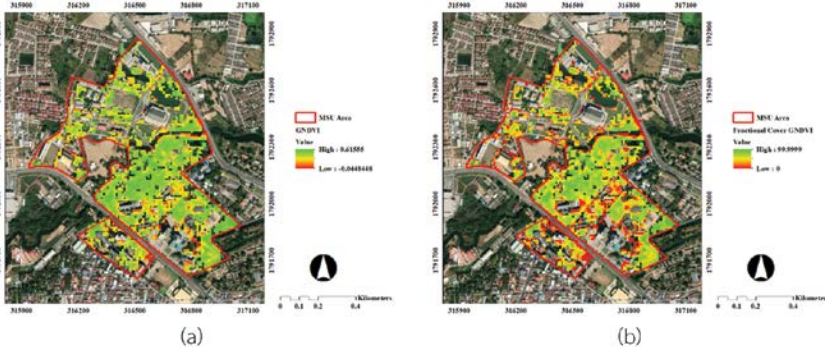


Figure 3 Satellite data analysis (a) GNDVI and (b) GNDVI-derived Fractional Cover

**Table 2** Fractional Cover

Sample Plot	Fractional Cover NDVI	Fractional Cover GNDVI
1	61.15	48.62
2	69.17	58.15
3	75.91	65.02
4	73.43	64.29
5	67.17	55.91
6	75.20	66.05
7	64.97	51.54
8	57.75	45.84
9	77.01	69.48
10	73.56	64.39
11	58.19	46.17
12	72.68	63.83
13	84.75	77.76
14	75.60	68.10
15	76.37	67.60
16	41.81	32.78
17	82.75	74.08
18	79.07	71.33
19	83.27	76.89
20	80.99	73.68
21	42.54	32.93
22	84.97	74.92
23	87.21	83.20
24	66.64	56.92
25	45.91	37.92
26	69.82	61.19
27	82.61	72.73
28	74.54	67.04
29	63.15	49.50
30	74.29	67.07

Table. 2 presents the Fractional Cover values for all 30 sample plots using various greenness indices, including NDVI (Normalized Difference Vegetation Index), and GNDVI (Green Normalized Difference Vegetation Index), to evaluate vegetation and associated soil conditions. From the analysis of the data in Table. 2, several patterns can be observed in the Fractional Cover values for each index, as follows:

NDVI: The average NDVI values ranged approximately from 41.81 to 87.21, with a mean value around 71.10, indicating a relatively high level of vegetation greenness across many plots.

GNDVI: The average GNDVI values ranged from approximately 32.78 to 83.20, with a mean of about 61.10, which is slightly lower than NDVI and shows a distribution pattern similar to NDVI.

The relationship among the indices—NDVI, and GNDVI—shows a similar distribution pattern, with GNDVI generally yielding slightly lower values compared to NDVI. This may indicate differences in how each index emphasizes the measurement of vegetation greenness. Plots with high Fractional Cover values, such as Plots 23, 19, and 22, suggest areas with lush vegetation and healthy plant conditions. Conversely, Plots 16 and 21 represent examples of plots with low Fractional Cover values across all indices, which may be due to factors such as poor tree health or water deficiency. The importance of using multiple indices lies

in enhancing the comprehensiveness of the analysis, as each index focuses on different aspects. Integrating data from multiple indices provides a more complete and clearer picture of the environmental conditions.

### 3.3 Correlation Analysis

From the analysis of the relationship between Fractional Cover (FC) and AGB using exponential regression, the results are presented in Figure. 4 (a) and (b). An analysis of the relationship between AGB density and fractional cover (FC) using exponential regression revealed that NDVI, and GNDVI have coefficients of determination ( $R^2$ ) of 0.6186, and 0.7201, respectively. Notably, GNDVI exhibited the highest correlation with an  $R^2$  value of 0.7201, and the resulting equation is  $y = 3.9972e^{0.0533x}$ . This equation indicates that the variability of AGB can be significantly explained by the FC calculated from GNDVI at a high level.

### 3.4 AGB Estimation

The AGB and carbon stock estimations derived from vegetation indices using exponential regression were calculated on a per-pixel basis. This was done by multiplying the biomass density per hectare by the area of one pixel (100 square meters), and then dividing by 10,000 square meters to convert the values to per-pixel units. The resulting raster layers represent biomass per pixel, as illustrated in Figure. 5 (a) and (b).

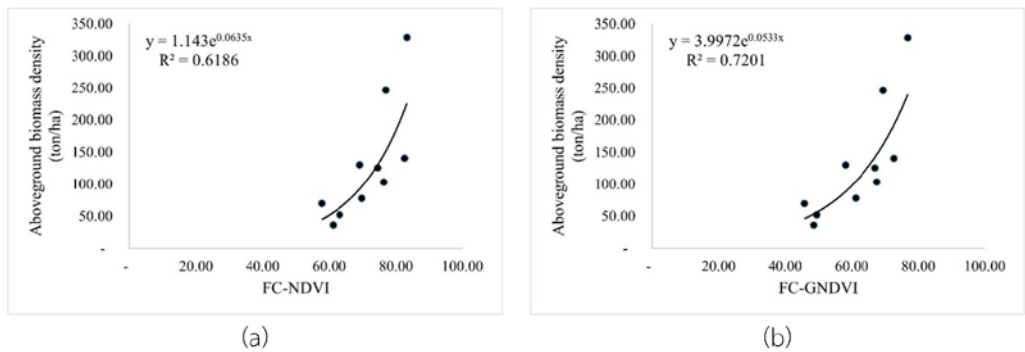


Figure 4 Correlation analysis (a) FC-NDVI, and (b) FC-GNDVI

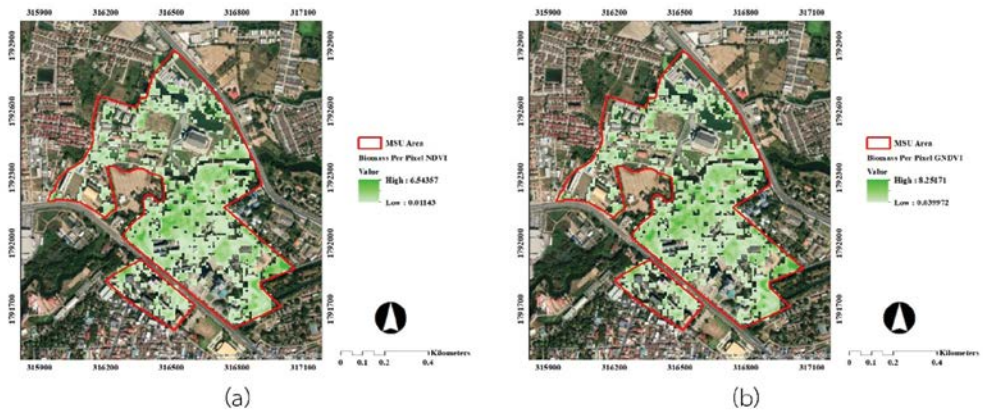


Figure 5 Aboveground biomass (a) FC-NDVI, and (b) FC-GNDVI

From Figure. 5 (a), the NDVI-based estimation shows that the maximum biomass in a 100 square meter area was 6.54357 tons, while the minimum was 0.01143 tons. The total biomass estimated from NDVI was 2,558.1196 tons. Figure.5 (b), presents the GNDVI-based estimation, with the highest biomass in a 100 square meter area being 8.25171 tons and the lowest 0.039972 tons. The total biomass calculated from GNDVI was 2,798.2262 tons. These results derived from NDVI, and GNDVI provide detailed and effective insights into the distribution

and quantity of AGB within the study area. The results of carbon stock derived from vegetation indices are illustrated in Figure. 6 (a) – (b).

Figure. 6 (a) presents the NDVI-based carbon stock. In a 100 square meter area, the maximum amount of sequestered carbon was 3.07548 tons of carbon, while the minimum was 0.0053721 tons of carbon. The total amount of carbon stock based on NDVI was 1,202.316209 tons of carbon. Figure.6 (b) shows the GNDVI-based carbon stock. The highest amount of carbon sequestered in a

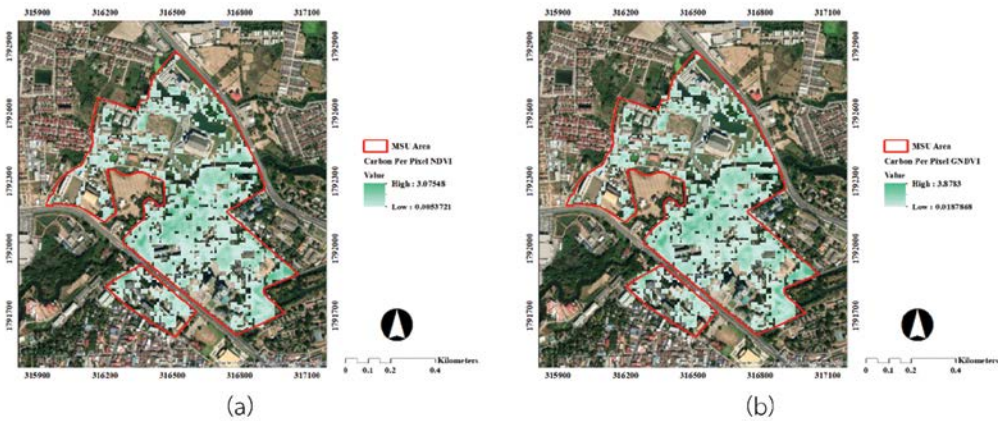


Figure 6 Carbon per pixel (a) NDVI, and (b) GNDVI

100 square meter area was 3.8783 tons of carbon, and the lowest was 0.00187868 tons of carbon. The total amount of carbon sequestered from GNDVI was 1,315.166321 tons of carbon. Figure.6 (b) shows the GNDVI-based carbon stock. The highest amount of carbon sequestered in a 100 square meter area was 3.8783 tons of carbon, and the lowest was 0.00187868 tons of carbon. The total amount of carbon sequestered from GNDVI was 1,315.166321 tons of carbon.

### 3.6 Statistical Accuracy Assessment

The results of the Root Mean Square Error (RMSE) and RMSE% calculations for evaluating the accuracy of biomass density estimates derived from satellite imagery compared with values obtained from field surveys are as follows:

NDVI: Based on the data analysis, the RMSE value calculated for NDVI was 2.36 tons per hectare (ton/ha), indicating that, on average, the satellite-derived biomass values

deviated from the field-based measurements by approximately 2.36 ton/ha. Additionally, the RMSE percentage (RMSE%) was calculated to be 44.99%, representing the percentage error relative to the actual field values.

GNDVI: The RMSE value calculated for GNDVI was 1.90 tons per hectare (ton/ha), which means that, on average, the satellite-derived values deviated from the field measurements by approximately 1.90 ton/ha. The corresponding RMSE% was 36.21%, indicating the percentage error relative to the actual values.

The relatively high RMSE% observed in this study—44.99% for NDVI and 36.21% for GNDVI—can be attributed to several factors inherent to both urban forest characteristics and the data source. First, urban plots exhibit structural heterogeneity, with diverse species, size classes, and canopy densities, which complicates the performance of single-index models calibrated on limited plot samples. Second, the 10 m spatial resolution of Sentinel-2 often produces mixed-pixel

effects, where individual pixels combine tree canopies with impervious or understory surfaces, thereby introducing systematic bias in spectral indices. Third, slight mismatches between plot boundaries and satellite footprints, along with phenological and management differences, further contribute to residual error. Previous studies have reported similarly high RMSE values when relying solely on Sentinel-2 indices, whereas the integration of canopy-height or LiDAR information has been shown to substantially reduce error, underscoring the importance of multi-source data integration. Therefore, future research should (i) stratify models according to vegetation type and structural characteristics, (ii) incorporate canopy-height metrics derived from UAV or LiDAR, and (iii) employ cross-validation approaches to more accurately characterize model generalization error.

#### 4. Conclusion

This study assessed aboveground biomass and carbon stock of urban trees at Mahasarakham University by integrating Sentinel-2 imagery with field surveys. Results showed that GNDVI was the most effective vegetation index, demonstrating a strong correlation with biomass estimation. Field surveys indicated a total biomass of 4,650.75 tons and carbon stock of 2,185.85 tons, while satellite-based analysis estimated 2,798.23 tons of biomass and 1,315.17 tons of carbon. These findings highlight the value

of combining space technology with ground measurements to provide accurate and scalable assessments of urban forest carbon potential. From a practical perspective, the results can inform urban green space planning by identifying high-biomass areas for conservation and management. Moreover, the quantified carbon stock provides baseline data for evaluating urban carbon credit opportunities. Future research should explore higher-resolution data, such as UAV or LiDAR, and expand the number of sample plots to further improve model accuracy and support evidence-based policies on climate change mitigation.

#### 5. Acknowledgement

This research project was financially supported by Mahasarakham University.

#### 6. Reference

- [1] A. T. Arevalo, "Climate change versus economic growth: Case of greenhouse apply a study of European Union countries and England from 2010 to 2019 using linear regression and neural networks," *Sustainability*, vol. 16, no. 5, Feb. 2024, Art. no. 1884.
- [2] M. Zubair, S. Chen, Y. Ma, and X. Hu, "A systematic review on carbon dioxide (CO<sub>2</sub>) emission measurement methods under PRISMA guidelines: Transportation sustainability and development programs," *Sustainability*, vol. 15, no. 6, Mar. 2023, Art. no. 4817.
- [3] T. Angkahad, W. Chokkuea, S. Sangpradid, Y. Uttaruk, K. Viriyasatr, and T. Laosuwan, "The assessment of aboveground biomass and carbon sequestration in community

- forests using UAV technology,” *Def. Technol. Acad. J.*, vol. 7, no. 15, pp. 11–28, Jan.–Apr. 2025.
- [4] Y. Uttaruk and T. Laosuwan, “Methods of estimation for above ground carbon stock in Nongbua-nonmee community forest, Maha Sarakham Province, Thailand,” *Agric. For.*, vol. 66, no. 1, pp. 183–195, 2020.
- [5] M. G. Muluneh, “Impact of climate change on biodiversity and food security: A global perspective—a review article,” *Agric. Food Secur.*, vol. 10, Oct. 2021, Art. no. 36.
- [6] United Nations, “Biodiversity - our strongest natural defense against climate change,” n.d. [Online]. Available: <https://www.un.org/en/climatechange/science/climate-issues/biodiversity>. Accessed: May 2, 2025.
- [7] U.S. Environmental Protection Agency, “Climate change impacts on ecosystems,” n.d. [Online]. Available: <https://www.epa.gov/climateimpacts/climate-change-impacts-ecosystems>. Accessed: May 3, 2025.
- [8] X. Yuan *et al.*, “Impacts of global climate change on agricultural production: A comprehensive review,” *Agronomy*, vol. 14, no. 7, Jun. 2024, Art. no. 1360.
- [9] M. S. Ragetti *et al.*, “Explorative assessment of the temperature–mortality association to support health-based heat-warning thresholds: A national case-cross-over study in Switzerland,” *Int. J. Environ. Res. Public Health*, vol. 20, no. 6, Mar. 2023, Art. no. 4958.
- [10] V. Heidt and M. Neef, “Benefits of urban green space for improving urban climate,” in *Ecology, Planning, and Management of Urban Forests*, M. M. Carreiro, Y. C. Song, and J. Wu, Eds. New York, NY, USA: Springer, 2008, pp. 84–96.
- [11] A. Woodward *et al.*, “Trees, climate change, and health: An urban planning, greening and implementation perspective,” *Int. J. Environ. Res. Public Health*, vol. 20, no. 18, Sep. 2023, Art. no. 6798.
- [12] Z. Rehman *et al.*, “Urban parks and native trees: A profitable strategy for carbon sequestration and climate resilience,” *Land*, vol. 14, no. 4, Apr. 2025, Art. no. 903.
- [13] W. Vattanavongsiri, S. Sangpradid, W. Chokkuea, and T. Laosuwan, “Estimation of above-ground carbon sequestration in the national reserved forest using vegetation indices and gradient boosting machine learning,” *Int. J. Tech. Phys. Probl. Eng.*, vol. 16, no. 3, pp. 361–366, Sep. 2023.
- [14] P. Saengpradit, S. Sangpradid, and T. Laosuwan, “Estimation of aboveground biomass using hybrid machine learning based on satellite imagery,” *Int. J. Tech. Phys. Probl. Eng.*, vol. 16, no. 4, pp. 7–13, Dec. 2024.
- [15] M. M. Rahman and J. Hasan, “Evaluating the impact of green spaces on urban heat reduction in Rajshahi, Bangladesh using the InVEST model,” *Land*, vol. 13, no. 8, Aug. 2024, Art. no. 1284.
- [16] T. Laosuwan, Y. Uttaruk, S. Nakapan, J. Itsarawisut, and C. Plybour, “Evaluation of tree biomass and carbon sequestration through remote sensing and field methods,” *Geogr. Tech.*, vol. 20, no. 1, pp. 33–43, Mar. 2025.
- [17] K. Al-Jabri *et al.*, “Integrating remote sensing techniques and allometric models for sustainable carbon sequestration

- estimation in *Prosopis cineraria*-Druce trees,” *Sustainability*, vol. 17, no. 1, Jan. 2025, Art. no. 123.
- [18] T. Rotjanakusol, S. Sangpradid, J. Itsarawisut, and T. Laosuwan, “Estimation of land surface temperature by derivative analysis of MOD11A2 product data, MODIS system,” *Def. Technol. Acad. J.*, vol. 2, no. 6, pp. 76–85, Jul.–Dec. 2020.
- [19] T. Angkahad *et al.*, “An empirical analysis of aboveground biomass and carbon sequestration using UAV photogrammetry and machine learning techniques,” *IEEE Access*, vol. 12, pp. 186740–186752, 2024.
- [20] T. Angkahad *et al.*, “Developing a drone-based machine learning for spatial modeling and analysis of biomass and carbon sequestration in forest ecosystems,” *ES Eng. Sci.*, vol. 35, 2025, Art. no. 1508.
- [21] S. Ullah *et al.*, “Multi-temporal and multi-resolution RGB UAV surveys for cost-efficient tree species mapping in an afforestation project,” *Remote Sens.*, vol. 17, no. 6, Mar. 2025, Art. no. 949.
- [22] H. Ogawa, K. Yoda, K. Ogino, and T. Kira, “Comparative ecological studies on three main types of forest vegetation in Thailand: II. Plant biomass,” *Nat. Life Southeast Asia*, vol. 4, pp. 49–80, 1965.
- [23] IPCC, *2006 IPCC Guidelines for National Greenhouse Gas Inventories*, S. Eggleston, L. Buendia, K. Miwa, T. Ngara, and K. Tanabe, Eds. Kanagawa, Japan: IGES, 2006
- [24] C. J. Tucker, “Red and photographic infrared linear combinations for monitoring vegetation,” *Remote Sens. Environ.*, vol. 8, no. 2, pp. 127–150, May 1979.
- [25] A. A. Gitelson, Y. J. Kaufman, and M. N. Merzlyak, “Use of a green channel in remote sensing of global vegetation from EOS-MODIS,” *Remote Sens. Environ.*, vol. 58, no. 3, pp. 289–298, Dec. 1996.
- [26] T. Laosuwan and P. Uttaruk, “Estimating tree biomass via remote sensing, MSAVI 2, and fractional cover model,” *IETE Tech. Rev.*, vol. 31, no. 5, pp. 362–368, Sep. 2014.
- [27] H. Yang and Z. Yang, “A modified land surface temperature split window retrieval algorithm and its applications over China,” *Global Planet. Change*, vol. 52, no. 1–4, pp. 207–215, Jul. 2006.
- [28] GM. Gebremichael and A. P. Barros, “Evaluation of MODIS gross primary productivity (GPP) in tropical monsoon regions,” *Remote Sens. Environ.*, vol. 100, no. 1, pp. 150–166, Jan. 2006.